

Pulsed field ionization of Rydberg atoms

F. Robicheaux

Department of Physics, Auburn University, Auburn, Alabama 36849

(Received 27 February 1997)

Fully quantum and classical trajectory Monte Carlo calculations are performed for a Rydberg alkali-metal atom that is kicked by a pulsed electric field. The two calculations are compared to recent experimental results through the ionization probability versus peak field strength. The energy distributions of the final electrons are compared between the two calculations. There is a qualitative difference between the classical and quantum momentum distributions which is measurable in principle. An experiment to detect the time-dependent precession of the orbital angular momentum in Cs is also proposed. [S1050-2947(97)51211-X]

PACS number(s): 32.80.Rm, 32.60.+i

Recent experimental and theoretical work has explored the dynamics of Rydberg alkali-metal atoms that are subjected to a kick from a unidirectional, pulsed electric field [1–13]. The pulses in these experiments are typically short compared to the Rydberg period of the electron. In this case, the electric field kicks the electron giving it an impulse in the field direction. Approximately, the only effect of this impulse is to change the electron's momentum in the field direction by an amount $\Delta\vec{p}$. This changes the electron's energy by an amount that depends on the momentum at the time of the pulse: $\Delta E = \Delta\vec{p} \cdot \vec{p} + (\Delta\vec{p})^2/2$. The electron may or may not escape the atom, depending on whether ΔE is larger or smaller than the binding energy of the initial state. This situation is in stark contrast to the dynamics in a static electric field where no states are bound, but the only question is, how fast does the electron tunnel and leave the atom?

In all of these papers describing kicked Rydberg atoms, the theoretical work has been restricted to classical calculations or to fully quantum calculations for states of $n \leq 17$. The classical calculations are performed by generating a distribution of trajectories with properties similar to the quantum state that is being kicked. The percentage of trajectories at positive energy after the kick is generally in very good agreement with the experiments. This is not too surprising since the initial state is a high Rydberg state and relatively little information about the final electron distribution is measured. We might expect that the dominant quantum effects, interference and tunneling, play a minor role in these measurements. It is the main purpose of this paper to directly compare fully quantum and classical trajectory Monte Carlo calculations to test the accuracy of the classical method. This will provide guidance as to what sort of accuracy needs to be obtained in order to measure the difference between classical and quantum mechanics in this system.

The second purpose of this paper is to address the interesting measurement scheme proposed by Jones [13]. In Ref. [13], it was shown how a pulsed electric field could be used to measure a component of the momentum distribution of a Rydberg state. Another secondary purpose of this paper is to show that the measured momentum distribution could be in better agreement with the actual distribution than was indicated in Fig. 1 of Ref. [13]. The method proposed by Jones is a difficult method to implement but could, in principle, be a

highly accurate method. With the accuracy that can be obtained, one could directly measure the precession of the orbital angular momentum in a Cs atom in the $27p$ state.

This method for measuring a component of the momentum distribution of a Rydberg electron has used the idea that within the impulse approximation the electron's change of energy is $\Delta E = \Delta p p_z + \Delta p^2/2$ where Δp is the impulse (assumed to be in the z direction) given to the electron. If the change in energy is greater than the binding energy ($E_B = -1/2\nu^2$), the electron will leave the atom. This means that the percentage of the atoms ionized, $P(p_z)$, equals the percentage of the electrons with the z component of the momentum larger than $p_z = (1/\nu^2 - \Delta p^2)/2\Delta p$. The experiment measures

$$P(p_z) = \int_{p_z}^{\infty} D(p'_z) dp'_z, \quad (1)$$

where $D(p_z)$ is the probability density for the electron to have momentum p_z and to have any value for p_x and p_y . The probability density may be obtained by differentiation of the measured $P(p_z)$:

$$D(p_z) = -\frac{dP(p_z)}{dp_z}. \quad (2)$$

This simple step points to the main difficulty in measuring the z component of the electron's momentum distribution: any experimental errors in measuring $P(p_z)$ become magnified when taking the difference that is needed to obtain $D(p_z)$. In Ref. [13], Jones showed that this method for measuring the momentum distribution works well enough to measure the oscillation of a wave packet on an atom. But it must be remembered that these equations are approximations. One purpose of this paper is to compare the exact momentum distribution to the distribution that would be measured in a perfect experiment similar to Ref. [13]. For this purpose, the time-dependent equations are accurately solved numerically to obtain the ionization probability after the pulse; the parameters $D(p_z)$ and $-dP(p_z)/dp_z$ are then compared. In fact, it is possible to distinguish between classical and quantum momentum distributions.

The quantum dynamics reduces to finding the solution of the time-dependent Schrödinger equation for one electron

with a time-dependent Hamiltonian given by $H(t) = H_{\text{atom}} + F(t)z$. H_{atom} is the effective one-electron atomic Hamiltonian for the Rydberg alkali-metal atom and $F(t)$ is the pulsed electric field. For all of the calculations $F(t)$ was chosen to have the form $F(t) = F_{\text{peak}} \exp[-4 \ln(2)t^2/\tau^2]$ where F_{peak} is the peak field strength and τ is the full width at half maximum (FWHM) of the pulse. The initial time in the calculations was chosen to be $t = -3\tau$ and the final time was $t = 3\tau$; with these choices the electric field has not turned on yet at the initial time and has completely turned off at the final time. At the initial time Ψ is set equal to the initial state, $\Psi(\vec{r}, -3\tau) = \psi_I(\vec{r})$.

We solved Schrödinger's equation by expanding $\Psi(\vec{r}, t)$ into a basis set of radial functions times spherical harmonics. The radial functions were eigenstates of the radial atomic Hamiltonian such that all of the functions go to zero at some fixed radial distance, r_f . The radial potential $V_\ell(r)$ is a model potential that was used to give the correct quantum defects in the Rydberg region; none of the calculated quantum defects differed from the experimental ones by more than 0.002. The second derivative in r was approximated using a five-point differencing method with the radial mesh points on a square-root mesh [14]. The radial orbitals could be obtained efficiently using a relaxation technique so that the calculation of orbitals and Hamiltonian matrix elements was a negligibly small part of the calculation.

Since the wave function is expanded in an orthonormal basis set, it is only necessary to time propagate the coefficients. The $C_{n\ell}(t)$ are defined by

$$\Psi(\vec{r}, t) = \sum_{n\ell} R_{n\ell}(r) Y_{\ell m}(\Omega) C_{n\ell}(t) / r. \quad (3)$$

The coefficients are solutions of the equation

$$\frac{\partial C_{n\ell}(t)}{\partial t} = -i \sum_{n'\ell'} H_{n\ell, n'\ell'}(t) C_{n'\ell'}(t), \quad (4)$$

where the Hamiltonian matrix elements are

$$H_{n\ell, n'\ell'}(t) = \epsilon_{n\ell} \delta_{nn'} \delta_{\ell\ell'} + F(t) \langle n\ell | z | n'\ell' \rangle. \quad (5)$$

The dipole matrix elements $\langle n\ell | z | n'\ell' \rangle$ were calculated numerically using a fifth-order integration scheme; the matrix elements between all n, ℓ and $n', \ell' \pm 1$ were computed to ensure the accuracy of avoided crossings between different n manifolds. A nice feature of this Hamiltonian is that it is block tridiagonal, so that a very large number of basis functions may be used without encountering storage problems on a workstation. This simple form obtains because we chose our basis set to be eigenstates of the atomic Hamiltonian with zero field. The time propagation in Eq. (4) was performed using the staggered leapfrog algorithm

$$\vec{C}(t + \delta t) = \vec{C}(t - \delta t) - 2i \delta t H(t) \vec{C}(t), \quad (6)$$

which is fairly accurate and easy to implement because it is an explicit method.

The most important idea that enables the calculation of the ionization probability has been glossed over. The trick is that the radial functions are obtained within a finite radial

distance r_f , so that *all* of the radial functions have the property $R_{n\ell}(r_f) = 0$. With this condition, there is no continuum; there are only discrete states. For low n , this condition does not perturb the quantum states. But as n increases, eventually the states can reach r_f and these states become perturbed. As n increases further, eventually $\epsilon_{n\ell}$ becomes greater than 0 and a whole sequence of discrete states in the positive-energy continuum is generated.

The cutoff radius is chosen to be large enough so that the initial state is easily contained within r_f ; the initial state is not perturbed by $R_{n\ell}(r_f) = 0$. The r_f must also be chosen to be large enough so that none of the wave function hits the r_f boundary before the pulse turns off. This condition is required because otherwise the final energy distribution of electrons is changed. For the calculations presented here, r_f was chosen to be 2500 a.u. The number of basis functions in each ℓ was $140 - \ell$ and the maximum ℓ was 100. It was necessary to go to large ℓ because the impulse can give an angular momentum of $r_{\text{max}} \Delta p = 2v^2 \Delta p$ to the electron; for the maximum field used in this study this gives a maximum angular momentum of 100. If the maximum angular momentum is not large enough, the electron will "reflect" from the barrier to excite high angular momentum (represented by not including high angular momentum in the basis) and will not ionize efficiently. For example, if the maximum angular momentum is reduced to ~ 50 , the ionization probability at 20 kV/cm is reduced by a factor of 2.

The calculation of the ionization probability can be performed using the coefficients $C_{n\ell}(3\tau)$. The ionization probability is simply the sum of the probabilities to be in each of the positive-energy states:

$$P = \sum_{n\ell} |C_{n\ell}(3\tau)|^2 \quad \text{for } \epsilon_{n\ell} > 0. \quad (7)$$

To obtain the distribution of final energies it is only necessary to calculate the probability for being in a state in a certain energy range. In these calculations the highest-energy basis function had energy 0.01 a.u. which is roughly double the energy of the highest-energy electron after being kicked by a 20-kV/cm half cycle pulse.

The classical calculations were performed by numerically solving the classical equations of motion for an electron with random initial conditions that match the quantum state. All trajectories start with energy equal to the binding energy of the 25d state of Na and all trajectories start with total angular momentum equal to 2.5 (the semiclassical d -wave angular momentum) and with $m = 0$. The random conditions on the orbit are obtained by starting $x(t_i) = r_o \cos \gamma$, $y(t_i) = 0$, and $z(t_i) = r_o \sin \gamma$, where r_o was always the outer radial turning point, γ is a randomly chosen number between 0 and 2π with a flat distribution, and $t_i = -3\tau - \beta \tau_{\text{Ryd}}$ (τ_{Ryd} is the Rydberg period and β is a randomly chosen number between 0 and 1 with a flat distribution). The initial velocity is completely determined by the initial position, ℓ and E , depending on whether the angular momentum in the y direction is positive or negative; the sign of the y component of the angular momentum was chosen randomly for each trajectory. The flat distributions in β and γ automatically produce the correct distribution in r , p_r , and θ at the true starting time

$t = -3\tau$. The codes were run for each of 100 different peak field strengths. After the field was off at $t = 3\tau$, the energy of the electron was determined. The probability for ionization was obtained by finding the percentage of the trajectories that finished at positive energy. The energy distribution was obtained by finding the percentage of trajectories with energies between $E - \delta/2$ and $E + \delta/2$. The classical and quantum final energy distributions were the same for the large value of δ that would be expected in an experiment.

Putting a reasonable bin of trajectories around the values of E , $|\vec{L}|$, and L_z (instead of using only the quantum values) does not change any of the qualitative features of the classical momentum distribution in the z direction. A reasonable bin in energy would extend from the average of the $24d$ and $25d$ energies to the average of the $25d$ and $26d$ energies; since the momenta scale like $1/n$, this would make a change in the momentum distribution of less than 2% ($[1/2] \times [1/25]$). A reasonable bin in L_z would extend from $-1/2$ to $1/2$. The momentum distribution in the z direction for $L_z \neq 0$ can be exactly obtained from the distribution for $L_z = 0$ by dividing the $L_z = 0$ distribution by $\sin\alpha$ and changing the scale of p_z by a factor of $\sin\alpha$, where α is the positive angle between the angular momentum vector and the z axis; since $\sin^2\alpha = 1 - L_z^2/\vec{L}^2$, the change in the distribution is less than 2% ($[1/8] \times [1/2.5^2]$). A reasonable bin in $|\vec{L}|$ would extend between $|\vec{L}| \pm 1/2$. The main change in the momentum distribution in the z direction arises from the change in the eccentricity of the orbit because the change in the radial velocity is negligible over most of the orbit; since the change in the eccentricity is E times the change in \vec{L}^2 , this gives a change in the distribution of less than 1%.

The main results of this paper relate to the behavior of the $25d$ $m=0$ state of Na kicked by a 500-fs electric-field pulse. The dynamics of the system for 100 peak field strengths between 0 and 20 kV/cm are obtained and used to “measure” the z component of the momentum distributions, as suggested by Jones. This is the same system used in Ref. [13].

In Fig. 1, the experimentally measured ionization probability versus peak field strength is shown with the solid line, and the theoretically measured probability is shown with the dashed line for the classical calculation and the dotted line for the quantum calculation. It is clear that all three of these curves are in substantial agreement with each other. This shows that the basic mechanism for ionization is correctly described in both the quantum and classical calculations. However, this is an integrated parameter. The differential parameter $D(p_z)$ shows a qualitative difference between the quantum and classical calculations.

In Figs. 2 and 3 are presented the main results of this paper. In Fig. 2, the classical momentum distribution for the $25d$ state is shown with the solid line and the measured distribution [using 10^5 classical trajectories per field and Eq. (2)] is shown with the dashed line. In Fig. 3, the quantum momentum distribution for the $25d$ state is shown with the solid line and the measured distribution (using $n_{\max} = 140$ and $\ell_{\max} = 100$) is shown with the dashed line. The quantum momentum distribution in the z direction (with p_x and p_y anything) for an $n/\ell/m$ state is given by

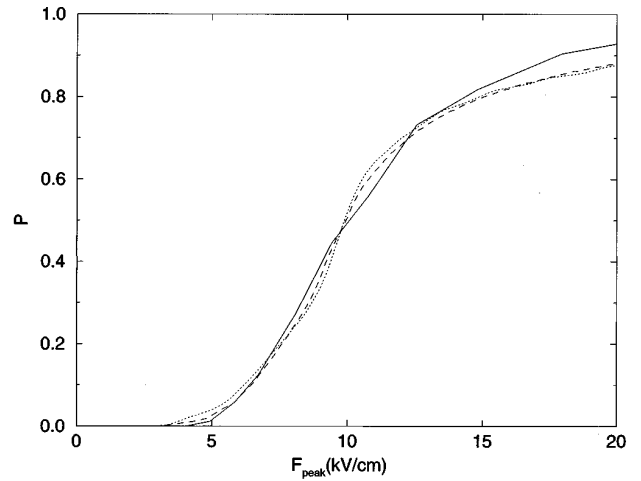


FIG. 1. Ionization probability versus peak field for a 0.5-ps FWHM pulse. Solid line, experimental results of Ref. [[13]]; dotted line, quantum calculation; dashed line, classical trajectory Monte Carlo calculation.

$$D(p_z) = 4 \int_0^\infty |Y_{\ell,m}(\cos\theta_p, 0)|^2 Q_n^2(p) p_\rho dp_\rho, \quad (8)$$

where $\cos\theta_p = p_z/\sqrt{p_z^2 + p_\rho^2}$ and $p = \sqrt{p_z^2 + p_\rho^2}$ and

$$Q_n(p) = \int_0^\infty j_\ell(pr) R_n(r) r dr. \quad (9)$$

Both the classical and quantum measurements were performed using a 500-fs FWHM pulse electric field. There were runs for 100 equally spaced peak field strengths from 0 to 20 kV/cm.

Several interesting features of these distributions are apparent. The most interesting is the qualitative difference between the classical and quantum distributions near $p_z = 0$: the classical distribution has a minimum and the quantum distribution has a maximum. This difference arises from the constructive interference at $p_z = 0$ for all states, such that $\ell + m$

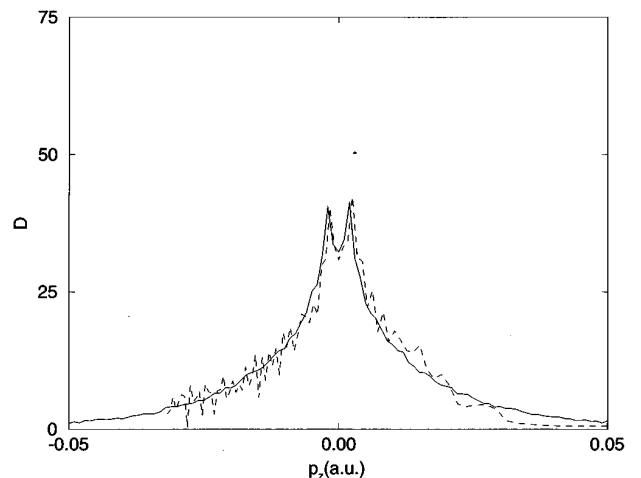


FIG. 2. Solid line, classical momentum distribution $D(p_z)$ in the z direction; dashed line, classical momentum distribution in the z direction as “measured” using $-dP(p_z)/dp_z$.

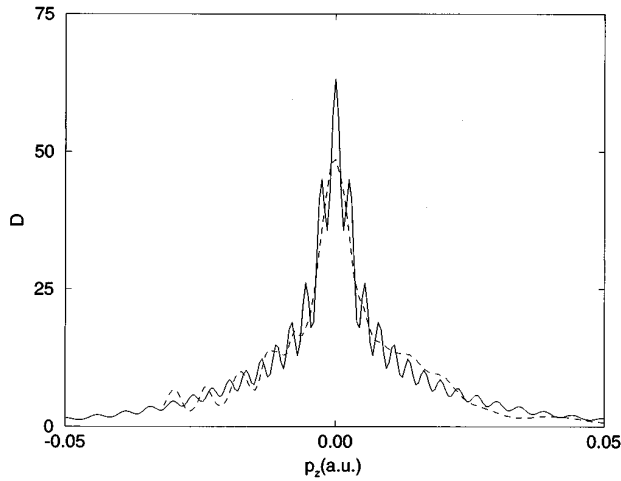


FIG. 3. Solid line; quantum momentum distribution $D(p_z)$ in the z direction; dashed line, quantum momentum distribution in the z direction as “measured” using $-dP(p_z)/dp_z$.

is even. When $\ell + m$ is odd, there is destructive interference and the distribution $D(p_z=0)=0$. This can be seen in Eq. (8) where the distribution at $p_z=0$ is given by

$$D(0) = 4 |Y_{\ell m}(\cos\theta=0, \phi=0)|^2 \left\langle \frac{1}{p} \right\rangle, \quad (10)$$

which equals

$$D(0) = \frac{(2\ell+1)(\ell+m)! (\ell-m)!}{2^{2\ell} (\ell!)^2 \pi} \frac{1 + (-1)^{\ell+m}}{2} \left\langle \frac{1}{p} \right\rangle. \quad (11)$$

Of course, the classical distribution does not have this property. For the $25d$ $m=0$ state, the constructive interference causes a very large maximum at $p_z=0$, whereas the classical distribution has a minimum. The important point of this distribution is that it is measurable in principle, using Jones’s method. The measured classical distribution shows a dip at $p_z=0$, while the quantum distribution is clearly peaked.

Another interesting feature is the noise in the classical distribution at negative p_z . This arises because the runs are

made using equal steps in the peak field strength. At the higher fields, this results in smaller steps in p_z . The statistical noise in going from one p_z to the next is enhanced. In the quantum distribution there is an oscillation in $D(p_z)$ for negative p_z whose source is completely unknown. This oscillation does not appear to be a numerical artifact: different runs with ℓ_{\max} increased by 20%, or n_{\max} increased by 20%, or r_f increased by 20%, or δt decreased by a factor of 2 all gave exactly the same results.

This interference effect in the quantum distribution is experimentally measurable, in principle, but of course the measurement will be difficult. For example, in the experiment of Ref. [13], the initial state, the $j=3/2$ state, was excited; this would wash out the interference effect at $p_z=0$ because the $j=3/2, |m_j|=1/2$ has both $m=0$ and $|m|=1$. One then might consider how to enhance this effect. One possibility would be to excite a Cs np state where $n \sim 20-30$, with a pulsed laser that has a pulse time much shorter than $2\pi/\Delta E$, where ΔE is the energy splitting of the $np_{3/2}$ and $np_{1/2}$ states. For $n=27$, $2\pi/\Delta E=61$ ps. If this excitation occurs with light linearly polarized in the z direction, the atom will be in a superposition of $np_{3/2}$ and $np_{1/2}$ states such that the spatial part of the packet will be purely $m=0$. Since $\ell+m$ is odd, the momentum distribution $D(p_z)$ will go to 0 at $p_z=0$. But after a time $\pi/\Delta E$, the spatial part of the wave function will be 89% in an $m=1$ or $m=-1$ state. Since $\ell+m$ is even, the momentum distribution will constructively interfere at $p_z=0$ and thus be substantially above the classical value. A bonus is that the precession of the orbit about the spin will be directly measurable.

In conclusion, classical and quantum calculations were performed for the Na $25d$ $m=0$ state kicked by a 500-fs electric-field pulse with peak field strengths from 0 to 20 kV/cm. It was shown that good agreement with experimentally measured ionization probabilities could be obtained. Perhaps, more importantly, it was shown that the method proposed by Jones could in principle distinguish between quantum and classical distributions. This method would allow the direct measurement of the orbit’s precession about the spin in Cs.

I greatly appreciate experimental data given to me by R.R. Jones and enlightening conversations with him. This work was supported by the NSF.

-
- [1] R.R. Jones, D. You, and P.H. Bucksbaum, Phys. Rev. Lett. **70**, 1236 (1993).
 [2] C.O. Reinhold, M. Melles, and J. Burgdörfer, Phys. Rev. Lett. **70**, 4026 (1993).
 [3] C.O. Reinhold, M. Melles, H. Shao, and J. Burgdörfer, J. Phys. B **26**, L659 (1993).
 [4] D. You, R.R. Jones, D.R. Dykaar, and P.H. Bucksbaum, Opt. Lett. **18**, 290 (1994).
 [5] C.O. Reinhold, H. Shao, and J. Burgdorfer, J. Phys. B **27**, L469 (1994).
 [6] K.J. LaGattuta and P.B. Lerner, Phys. Rev. A **49**, R1547 (1994).
 [7] R.R. Jones, N.E. Tielking, D. You, C.S. Raman, and P.H. Bucksbaum, Phys. Rev. A **51**, 3370 (1995).
 [8] N.E. Tielking, T.J. Binsky, and R.R. Jones, Phys. Rev. A **51**, 3370 (1995).
 [9] N.E. Tielking and R.R. Jones, Phys. Rev. A **52**, 1371 (1995).
 [10] A. Bugacov, B. Piraux, M. Pont, and R. Shakeshaft, Phys. Rev. A **51**, 1490 (1995); **51**, 4877 (1995).
 [11] C. Raman, C.W.S. Conover, C.I. Sukenik, and P.H. Bucksbaum, Phys. Rev. Lett. **76**, 2436 (1996).
 [12] M.T. Frey, F.B. Dunning, C.O. Reinhold, and J. Burgdörfer, Phys. Rev. A **53**, R2929 (1996).
 [13] R.R. Jones, Phys. Rev. Lett. **76**, 3927 (1996).
 [14] F. Robicheaux and J. Shaw, Phys. Rev. A **56**, 278 (1997).